Journal of Sound and Vibration (2001) **242**(5), 893–905
doi:10.1006/jsvi.2000.3395, available online at http://www.idealibrary.com on IDEAL®

PHASE DRIFT CHARACTERISTICS OF SELF-EXCITED, COMBUSTION-DRIVEN OSCILLATIONS

T. C. Lieuwen

School of Aerospace Engineering Georgia Institute of Technology Atlanta, GA 30332-0150, *U.S.A.*
E-mail: tim.lieuwen@aerospace.gatech.edu

(*Received* 30 *May* 2000; *and in final form* 25 *September* 2000)

This paper describes an experimental characterization of the phase drift characteristics of the oscillating pressure in an unstable combustor. It is shown that the phase continuously drifts in a predominantly irregular manner and, given enough cycles, substantially drifts from its "initial" value. It is also shown that the mean-squared value of the phase drift monotonically increases with the number of cycles, a result that is consistent with the predictions of a random walk model. It is concluded that these phase drift characteristics are primarily caused by random processes (i.e., noise) and, thus, do not reflect the underlying low-dimensional dynamics of the instability.

1. INTRODUCTION

The occurrence of detrimental instabilities in lean, premixed (LP) combustors continues to hinder the development of modern gas turbines [1–3]. These instabilities arise from interactions between oscillatory flow and heat release processes in the combustor and often lead to large amplitude, organized oscillations of the combustor's flow fields. These oscillations are undesirable because they significantly reduce the lifetime and regions of operability of the combustor.

In an effort to eliminate these instabilities, a number of studies of the mechanisms responsible for their occurrence and approaches for their control have been performed during the past few years [1–9]. Several of these studies have shown that these instabilities are likely initiated by a mechanism involving interactions between heat release, pressure, and reactive mixture composition oscillations [3–8].

As emphasized by Culick and coworkers [10–13], however, an understanding of the mechanism that is responsible for an instability does not necessarily provide any information about the processes that control the nonlinear oscillations of the system. Such an understanding of the transient and steady state non-linear oscillatory characteristics of unstable combustors is needed to, for example, predict the amplitude of the oscillations or develop and optimize active-control systems [7, 9].

The role of non-linear combustor processes in initiating and sustaining combustion instabilities has been and continues to be a subject of theoretical investigations; e.g., see references [10–17]. These analyses have yielded a great deal of insight into the complex non-linear behavior that is often observed in unstable combustors. For example, they have demonstrated the existence of stable limit cycles in unstable combustors or the possibility of "triggering" of instabilities in linearly stable systems [11, 13].

0022-460X/01/200893 + 13 $35.00/0

There has been little direct comparison, however, of the predictions of these analyses with experimental results. Furthermore, although there are numerous experimental combustion instability studies in the literature [1–7, 18–21], there has been little explicit treatment of the non-linear processes that control the combustor oscillations in these studies. As such, there has been little convergence of theoretical predictions and experimental results that would allow for a critical assessment of the accuracy and completeness of the current understanding of the non-linear processes that affect the oscillations in unstable combustors.

This and a companion paper [22] report the results of studies that analyzed pressure data measured in an unstable combustor in an effort to elucidate the characteristics of the non-linear system dynamics. In pursuit of this goal, the work described in this paper investigated the *cyclic variability in the phase* of the pressure oscillations. This work was motivated by the observation that combustion instabilities are typically manifested as nearly harmonic, low-degree-of-freedom oscillations of the combustor pressure. While these harmonic oscillations are very repeatable (e.g., autocorrelations of the combustor pressure often retain values of near unity for several hundred cycles), they also exhibit cycle-to-cycle variability, similar to that observed in, for example, other unstable combustors [19–21] and internal combustion engines [23]. This work investigates the cycle phase variability in an effort to determine whether it can be used to obtain information about the underlying processes that control the non-linear dynamics of the system.

To meet this goal, it is first necessary to determine whether such cyclic variability arises from the non-linear processes controlling the low-degree-of-freedom oscillations that are of interest, or from "background noise" (e.g., turbulent fluctuations) that is essentially stochastic in nature [24, 25]. In other words, it is necessary to determine whether the cyclic variability actually reflects the dynamics of the low-degree-of-freedom combustion instability, or is due to "background noise". If the effects of noise are too large, then steady-state limit cycle data may not provide any information about the non-linear characteristics of these systems.

The results of this investigation are presented in the following manner: The next section presents experimental data and characterizes the main features of the cycle-to-cycle variability in the phase of the pressure oscillations. Section 3 considers whether an underlying low-dimensional system dynamic is reflected in these data. Section 4 suggests that the majority of the phase drift is due to essentially random processes and, thus, does not reflect the underlying dynamics of the combustion driven oscillations.

2. ANALYSIS OF COMBUSTOR PRESSURE DATA

The data presented in this paper were measured during unstable operation of a lean, premixed gas turbine combustor simulator, see Figure 1, that is described in detail in reference [6]. The natural longitudinal acoustic frequencies of the system are approximately multiples of 100 Hz (i.e., 100, 200, … , Hz) and excitation of the first seven of these modes have been observed under different test conditions [6]. The data presented below were obtained during a 204 Hz instability that was sampled over 13 000 consecutive cycles at a sampling frequency of 2000 Hz with a transducer located in the combustor. Table 1 summarizes the operating conditions under which these data were obtained.

As stated above, this study investigated the cycle-to-cycle variability of the phase of pressure oscillations and, particularly the "drift" of this phase. This drift is illustrated in the data presented in Figure 2. Figure 2 compares a time series record of measured pressure data with an "average" harmonic signal given by $S(t) = A\cos(2\pi ft + \phi)$ whose amplitude,

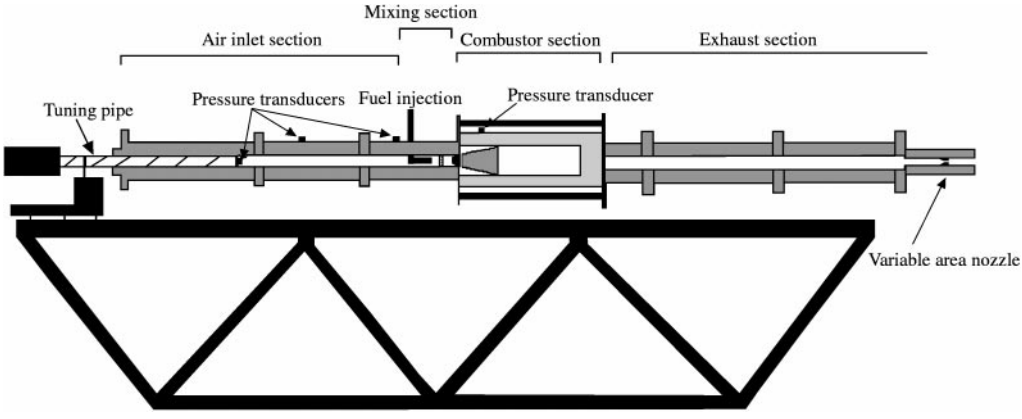

Figure 1. A schematic of the investigated lean, premixed combustor simulator.

TABLE 1

Summary of combustor operating conditions

Mean inlet section velocity u (m/s)	Mean combustor pressure (atm)	Oscillatory pressure amplitude (kpa)
14·2	6·78	4280
14·5	6·68	3180
14·6	6·60	3440

Note: All data were obtained at an equivalence ratio of $\phi = 0{\cdot}85$ and a total mass flow rate of 16 g/s.

A, and frequency, f, were determined by calculating their average values over 13 000 cycles of oscillation. The phase, ϕ, was set to equal the phase of the data during the first several cycles of oscillation. As shown in Figure 2(a) the harmonic signal and measured data coincide almost exactly for the initial four cycles of oscillation. A comparison of the harmonic signal with the data after 100 cycles of oscillation shows, however, that the phase, ϕ, has drifted approximately 45°. Although not shown here, an examination of the phase at later cycles shows that it drifts irregularly and, given enough cycles, appears to take all values between 0 and 360° with uniform probability.

The rest of the results presented in this section further quantify the phase drift that is shown in Figure 2. It was evaluated by determining the temporal locations of the zero crossings of the measured pressure data using linear interpolation. Using this technique, the phase can be estimated within an uncertainty of $-0{\cdot}7$–$1{\cdot}4°$.

Note that using zero crossings as an indicator of phase is only valid if the oscillatory signal is dominated by a single frequency component. This is the case for the data presented below, as Fourier transforms of the pressure data indicate, see Figure 3, that the next largest periodic components in the measured signal are 404 and 808 Hz oscillations with amplitudes that are approximately 30 times smaller than the 204 Hz oscillations. These frequency components are likely the harmonics of the 204 Hz mode that are excited by system non-linearities (the fact that they are not exact multiples in the Fourier transform is likely due to errors derived from finite sample lengths).

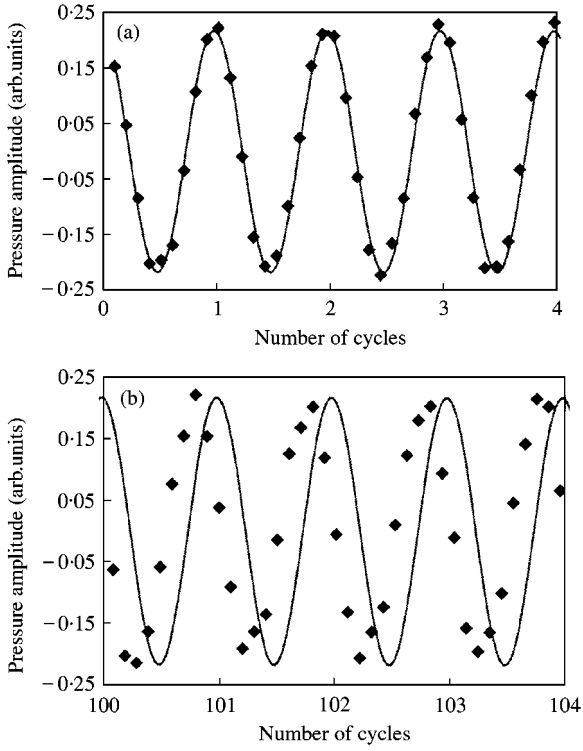

Figure 2. Comparison of measured combustor data (◆) with the signal $A\cos(2\pi ft + \phi)$ (—) for (a) the first 4 cycles and (b) after 100 cycles.

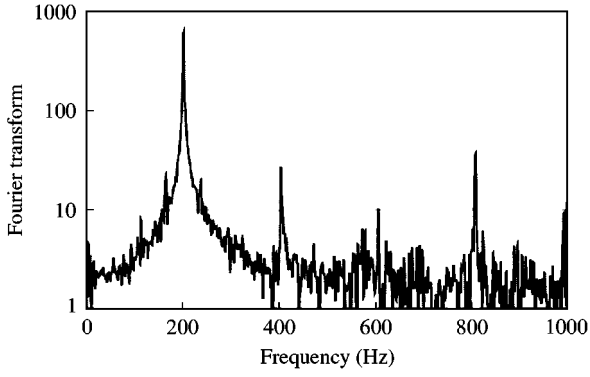

Figure 3. Fourier transform of the combustor pressure for the data shown in Figure 2.

Note that the difference between successive zero crossings approximately equals half a period of oscillations. As might be expected, however, this time difference takes a range of values in the data. The statistical characteristics of this time difference are illustrated by its probability density function (PDF) in Figure 4. Figure 4 indicates that the PDF of the distance between zero crossings is nearly Gaussian. The average time between zero crossings shown in Figure 4 is 2·45 ms, corresponding to an instability with a frequency of $f = 0{\cdot}5/0{\cdot}00245 = 204$ Hz. The standard deviation of the time between zero crossings is 0·042 ms, which corresponds to a standard deviation of the phase drift $\sigma_d = 360{*}0{\cdot}042/2{\cdot}45 = 6{\cdot}17^\circ$ per half cycle. The corresponding values of σ_d for the tests

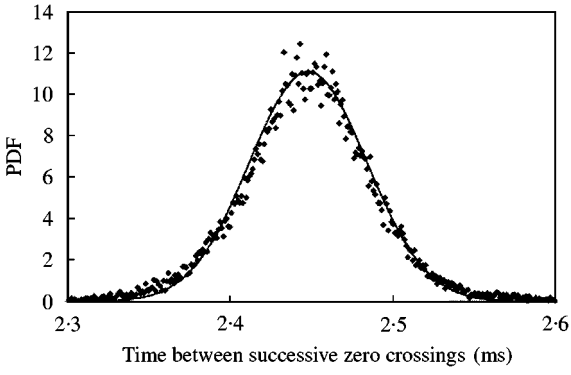

Figure 4. Comparison of the probability density function of the time between successive zero crossings (◆) and a Gaussian distribution ($u = 14{\cdot}5$ m/s) (—).

conducted with the mean inlet section velocities of $u = 14{\cdot}2$ and $14{\cdot}6$ m/s cases (see Table 1) are $6{\cdot}38$ and $5{\cdot}81^\circ$ per half cycle, respectively.

Using the locations of the zero crossings of the pressure signal, the following procedure was employed to divide the complete data record, composed of a total of N cycles, into ensembles and to determine the dependence of the phase drift upon the number of cycles for each ensemble: (1) determine the average time between every other zero crossing, $\bar{T}$ (i.e., the period of oscillations), of the entire data record, (2) divide the data record into k ensembles, where each ensemble is composed of $n = N/k$ cycles of data (where n and k are integers), (3) define the time from the beginning of the ith data record to the location of the $2j$th zero crossing (i.e., the jth cycle) as $t_{j,i}$ (where $j = 1, 2, \ldots, n$, and $i = 1, 2, \ldots, k$), (4) define the difference between $t_{j,i}$ and the location of the "average" zero crossing, $j\bar{T}$ by $d_{j,i} = t_{j,i} - j\bar{T}$, (5) define the phase drift after the jth cycle as $q_{j,i} = 360 d_{j,i}/\bar{T}$ degrees. Note that $\sum_{i=1}^{k} d_{j=n,i} = \sum_{i=1}^{k} q_{j=n,i} = 0$ by definition, because all phases are referenced to the average period, $\bar{T}$.

Figure 5 plots the typical dependence of the phase drift, $q_{j,i}$ upon the number of cycles, j ($u = 14{\cdot}5$ m/s, $k = 50$ ensembles). For clarity, the figure only illustrates phase drift data for six out of the 50 ensembles, Several items should be noted from the figure. First, the figure shows that the phase does not simply oscillate about its initial value. Rather, it exhibits a net drift that, in general, increases with the number of cycles. Second, there is no obvious similarity or relationship between the phase drifts exhibited by different ensembles. For example, the phase in some ensembles drifts very slowly and in other drifts much more rapidly. Third, the phase drift exhibited by some of the ensembles displays oscillatory characteristics, while that in other ensembles monotonically diverges from its initial value. Thus, an examination of these data does not indicate the presence of any easily discernable pattern or structure of the phase drift characteristics.

The possible presence of an underlying pattern in the data has been further examined by comparing the extent to which phase variability at a certain time is correlated with the phase variability at previous times. This relationship was examined using the following expression for the autocorrelation of $q_{j,i}$ (where $k = 1$ so the subscript i in $q_{j,i}$ is dropped):

$$C_s = \frac{\sum_{j=1}^{N/2} q_j q_{j+s}}{\sum_{j=1}^{N/2} (q_j)^2}, \quad s = 0, 1, \ldots, N/2. \tag{1}$$

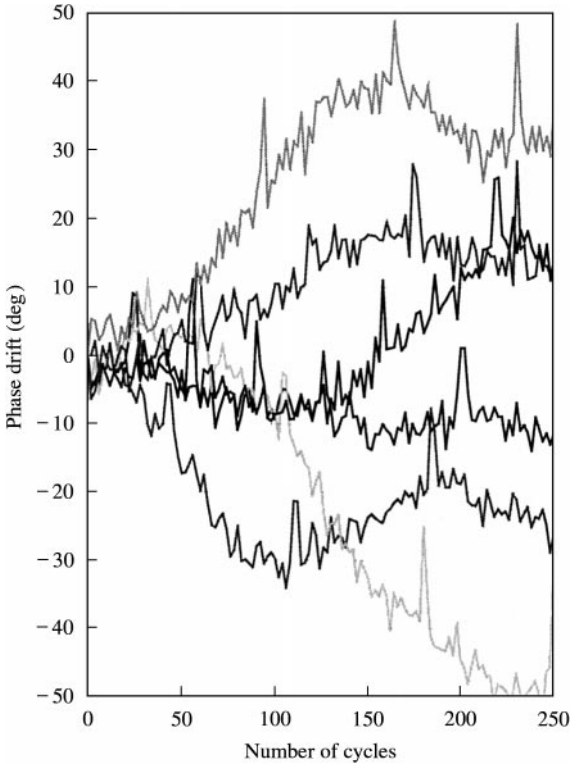

Figure 5. Comparison of the measured dependence of the phase drift of the combustor pressure upon the number of cycles at six different sections of the data record ($u = 14{\cdot}5$ m/s).

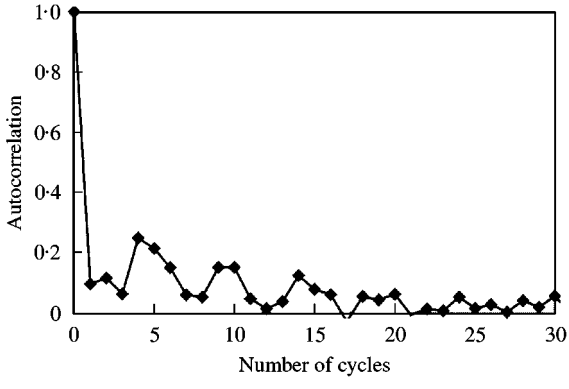

Figure 6. Dependence of the autocorrelation of the phase variability upon the number of cycles ($u = 14{\cdot}5$ m/s).

C_s quantifies the correlation between the phase deviation at some instant and its deviation s cycles later. Figure 6 illustrates the typical dependence of C_s upon the number of cycles and shows that there is almost no correlation of q_j with itself, *even after one cycle*. This lack of correlation suggests that much of the phase drift shown in Figure 5 arises from processes with short "memories" relative to the period of the pressure oscillations; i.e., processes that can be idealized as random.

To further analyze the phase variability shown in Figure 5, ensemble averages of the phase drift data were examined, i.e., the averaged values of $q_{j,i}$ over all k ensembles (where $i = 1, 2, \ldots, k$). Rather than examining the average value of the phase drift itself (because its average value at the nth cycle is zero by definition; i.e., $(1/k)\sum_{i=1}^{k} q_{j=n,i} = 0$, see above), however, it is more useful to examine the mean-squared phase drift:

$$\overline{q_j^2} = \frac{1}{k} \sum_{i=j}^{k} (q_{j,i})^2. \tag{2}$$

The objective behind the ensemble averaging procedure is to determine what type of behavior the "average" data exhibits. There is an important point that should be noted about this procedure, however, because it introduces the parameter k whose "correct" or "optimum" value is unknown. In other words, it is desirable to examine the average characteristics of the phase drift over as large a number of cycles as possible. This implies that the value of n should be large, which for a fixed number of measured cycles of data, N, requires a *small* value of $k = N/n$. In order to have good confidence in the averaged data, however, it is necessary to ensemble average over a large number of data sets, i.e., to have a *large* value of k.

Because of the tradeoff noted above, results are presented for several values of k. The results for the lower values of k provide information on the average phase drift behavior over long-time scales. Because these data are obtained by averaging over a small number of ensembles, reduced confidence can be placed in evaluations of whether any apparent patterns in the data are deterministic or random in origin. The results for higher k values provide information that higher confidence can be placed in, but only over shorter time scales. Figure 7 illustrates ensemble averaged phase drift plots for $k = 30$, 75, and 150. The figure shows that the mean-squared phase drift monotonically increases with the number of cycles. This result shows that the oscillatory phase does not remain about its initial value but rather, it diverges from its initial value. Figures 7(b) and (c) also show that, neglecting the first 20 cycles, the mean-squared phase drift exhibits a nearly linear dependence upon the number of cycles. Finally, Figure 7 shows that the rate of phase drift is largest and smallest in the $u = 14{\cdot}2$ and 14·6 m/s cases respectively. This result suggests that the rate of phase drift correlates with σ_d (i.e., the variability of the distance between successive zero crossings) because the highest rates of phase drift correspond to the highest values of σ_d and *vice versa* (recall that the values of σ_d for the $u = 14{\cdot}2$, 14·5 and 14·6 m/s cases were 6·38, 6·17, and 5·81° per half cycle respectively).

Besides the monotonically increasing phase drift, the phase data presented in Figure 7 also displays some oscillatory characteristics. These oscillatory characteristics manifest themselves as slow time-scale oscillations that are best seen in the phase drift behavior over a large number of cycles in Figure 7(a). These oscillatory characteristics can also be seen by examining the difference between the data shown in Figure 7(a) and a least-square cubic fit through the data (the choice of a cubic fit is arbitrary); see Figure 8. All three subplots in Figure 8 show that the phase drift has oscillatory characteristics (with an oscillatory period of approximately 150 cycles $\sim$1·4 Hz). Note, however, that the amplitude of the oscillations are quite small relative to the overall monotonic increase of the mean-squared phase drift shown in Figure 7.

3. DISCUSSION

This section examines whether the phase drift characteristics presented in the previous section are controlled by low-degree-of-freedom non-linear system dynamics or by the

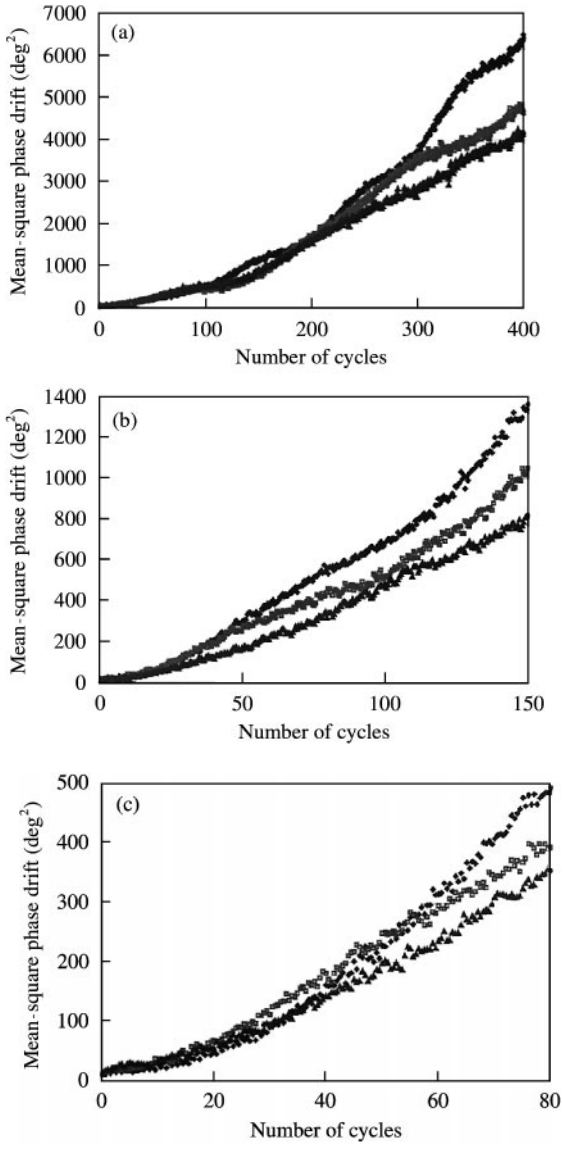

Figure 7. Dependence of the mean-squared phase drift upon the number of cycles for three different combustor operating condition and k values of (a) 30, (b) 75, and (c) 150. In all three subplots, the data were obtained at a mean inlet velocity of 14·2 m/s (top curve), 14·5 m/s (middle curve), and 14·6 m/s (bottom curve).

essentially random disturbances imposed on the system by, for example, turbulent fluctuations. To address this question, we have considered what type of results would be expected if the phase drift were due to random processes. It will be shown that the majority of the ensemble averaged phase drift characteristics described in the prior section can be captured by a random walk model.

The basic assumption behind the random walk model is that the phase drift at any cycle, q_j, is equal to its value at the prior cycle, q_{j-1}, plus a perturbation, M_j, i.e. $q_j = q_{j-1} + M_j = \sum_{m=1}^{j} M_m$. This perturbation could be due to, for example, turbulent fluctuations in velocity or temperature. We also assume that there is an uncertainty in

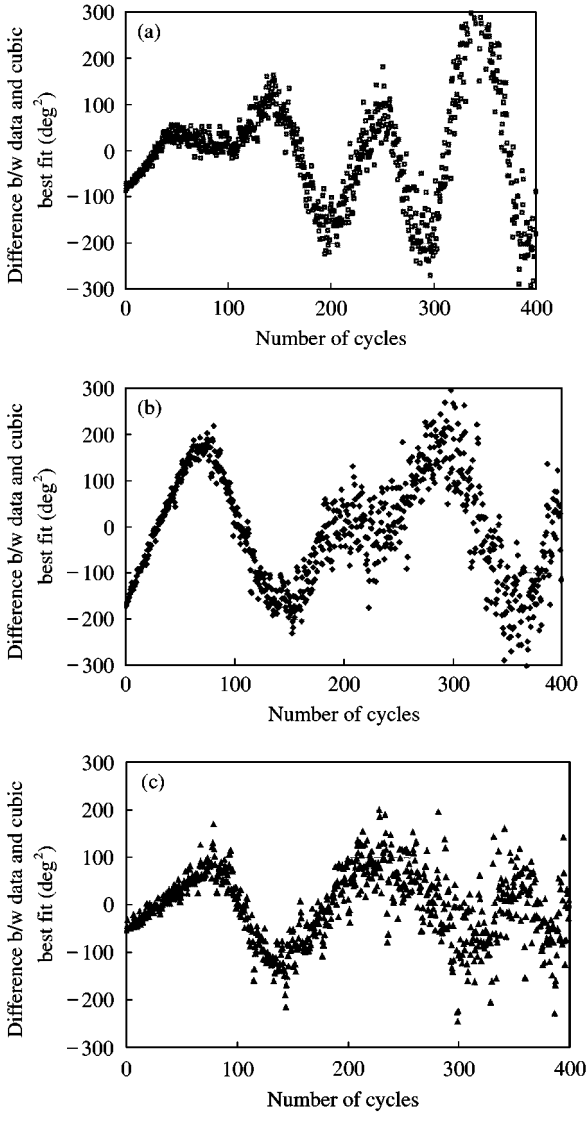

Figure 8. Difference between the data shown in Figure 7(a) and a cubic fit through the same data. Data were obtained at a mean inlet velocity of (a) $u = 14{\cdot}2$ m/s (b) $u = 14{\cdot}5$ m/s, (c) $u = 14{\cdot}6$ m/s.

determining the phase drift that is given by A_j. The resultant stochastic model for the phase drift is

$$q_j = A_j + \sum_{m=1}^{j} M_m. \tag{3}$$

A_j and M_m describe random system disturbances with zero mean and variances of σ_A^2 and σ_M^2 respectively. Note that these disturbances have qualitatively different effects upon the characteristics of q_j. A_j represents processes that introduce a purely additive component to the phase drift while M_j represents those processes that can accumulate. Note that the total drift, q_j, after j cycles (or "walks") is a function of all the multiplicative components in the

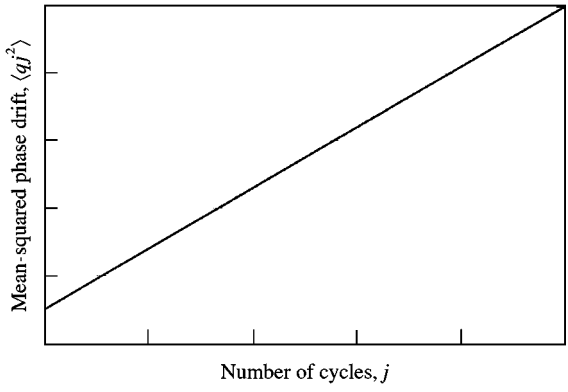

Figure 9. Predicted dependence of the mean-squared phase drift upon the number of cycles obtained with a random walk model. The slope of the line is σ_M^2.

past, i.e., $M_1, M_2, \ldots, M_j$, and is only a function of the immediate value of the additive component, A_j. Assuming that $A_j, M_1, M_2, \ldots, M_j$ are stationary, satistically independent† random processes, it can be shown that the expected value of the mean-squared phase drift equals [26]

$$\langle q_j^2 \rangle = \langle A_j^2 \rangle + \sum_{m=1}^{j} \langle M_m^2 \rangle = \sigma_A^2 + j\sigma_M^2, \tag{4}$$

where $\langle\ \rangle$ denotes the expected value operator. Figure 9 plots the predicted characteristics of $\langle q_j^2 \rangle$ and shows its predicted linear dependence upon j, the number of cycles. Thus, the figure and equation (4) show that *purely random processes can cause a monotonically increasing mean-squared phase drift*. While the simple random walk model given by equation (3) predicts a linear dependence of $\langle q_j^2 \rangle$ upon j, it is possible to consider more complex random models that predict a non-linear dependence between these two quantities (e.g., see reference [26]).

While the predictions of equation (4) do not completely describe the characteristics of the data shown in Figure 7, a comparison of the two shows that the model does capture many of its dominant features. Specifically, the monotonically increasing drift in phase of the data shown in Figure 7 is completely consistent with the predictions of equation (4). Second, the mean-squared phase drift obtained by averaging over a large number of cycles (shown in Figure 7(c) exhibits a nearly linear dependence upon the number of cycles between $j = 20$ and 80 cycles, in agreement with the predictions of equation (4). While this agreement does not constitute conclusive proof, it does show that the observed phase drift characteristics are consistent with those that would be expected if they were due to random processes.

It should be pointed out that while the *dominant* measured phase drift characteristics are consistent with the predictions of a random model, it is likely that there is some manifestation of deterministic processes in the approximately 1·4 Hz oscillations of the

†If $M_1, M_2, \ldots, M_j$ are not statistically independent (i.e., a "correlated" walk) but the area underneath he autocorrelation curve is finite (i.e., the area under the curve in Figure 4), then it can be shown that $\langle q_j^2 \rangle$ still increases linearly with j, but with a modified slope [26].

phase shown in Figure 8. Specifically, Figure 8 indicates that the phase drift exhibits a small amount of *repeatable oscillatory* behavior that is evident over long-time scales. While these results must be interpreted with care since they were obtained from ensemble averaging only 30 records (i.e., $k = 30$), the presence of oscillatory characteristics in all three of the results, taken at different times and operating conditions, suggests that this periodicity is not accidental. A number of combustor processes could be responsible for these slow oscillations. For example, they could arise from non-linear combustor processes that cause a slow "breathing" of the phase or from a slow oscillation in the fuel or air control system.

4. CONCLUSIONS

This paper describes an analysis of the characteristics of cycle-to cycle variability in the phase of the oscillatory pressure during combustion instabilities. Its principal findings and conclusions are as follows: (1) the phase of the oscillatory pressure during a combustion instability varies from cycle-to-cycle and, given enough cycles substantially drifts from its "initial" values; (2) the mean-squared value of the phase drift increases monotonically with the number of cycles; (3) the dominant features of the measured phase drift are consistent with the predictions of a random walk model, suggesting that it is due to "background noise"; (4) deterministic processes may be responsible for small amounts of periodicity in the phase drift that are evident over long-time scales, i.e., over time scales of the order of 150 cycles of oscillation. These findings are also consistent with those of Culick *et al.* [24] and Burnley [25], who suggest that unsteady motions in unstable combustors are composed primarily of low dimensional oscillations upon which high dimensional, random-like characteristics are superposed.

Also, this paper's demonstration that the phase of the oscillatory pressure continuously drifts during an instability implies that efforts to actively suppress combustion instabilities must take this phase drift into account by designing controllers that can sense, identify, and perform the necessary actuation over faster time scales than that of the phase drift. Otherwise, the phase of the control actuation will not be optimally phased to suppress the oscillations.

ACKNOWLEDGMENTS

This research was partially supported by AGTSR under contract # 99-01-SR075.

REFERENCES

1. J. COHEN and T. ANDERSON 1996 *American Institute of Aeronautics and Astronautics Paper* # 96-0819. Experimental investigation of near-blowout instabilities in a lean premixed combustor.
2. J. C. BRODA, S. SEO, R. J. SANTORO, G. SHIRHATTIKAR and V. YANG 1998 *Twenty-Seventh (International) Symposium on Combustion.* Pittsburgh: The Combustion Institute. An experimental study of combustion dynamics of a premixed swirl injector.
3. D. L. STRAUB and G. A. RICHARDS 1998 *American Society of Mechanical Engineers Paper* # 98-*GT*-492. Effect of fuel nozzle configuration on premix combustion dynamics.
4. T. LIEUWEN, H. TORRES, C. JOHNSON and B. T. ZINN 1999 *ASME paper* # 99-*GT*-003. A mechanism of combustion instability in lean premixed gas turbine combustors.
5. M. C. JANUS, G. A. RICHARDS and M. J. YIP 1997 *American Society of Mechanical Engineers Paper* #97-*GT*-266. Effects of ambient conditions and fuel composition on combustion stability.

6. H. TORRES, T. LIEUWEN, C. JOHNSON, B. R. DANIEL and B. T. ZINN 1999 *American Institute of Aeronautics and Astronautics Paper # 99-0712*. Experimental investigation of combustion instabilities in a gas turbine combustor simulator.
7. A. A. PERACCHIO and W. M. PROSCIA 1998 *American Society of Mechanical Engineers Paper # 98-GT-269*. Nonlinear heat release/acoustic model for thermo-acoustic instability in lean premixed combustors.
8. T. LIEUWEN and B. T. ZINN 1998 *Twenty-Seventh (International) Symposium on Combustion, The Combustion Institute, Pittsburgh*. The role of equivalence ratio oscillations in driving combustion instabilities in low NO_x gas turbines.
9. T. POINSOT, D. VEYNANTE, F. BOURIENNE, S. CANDEL, E. ESPOSITO and J. SURGET 1988 *Twenty Second Symposium (International) On Combustion. The Combustion Institute, Pittsburgh*. Initiation and suppression of combustion instabilities by active control.
10. C. C. JAHNKE and F. E. C. CULICK 1994 *Journal of Propulsion Power* **10**. An application of dynamical systems theory to nonlinear combustion instabilities.
11. F. E. C. CULICK, V. BURNLEY, and G. SWENSON 1995 *Journal of Propulsion Power* **11**. Pulsed instabilities in solid-propellant rockets.
12. V. YANG, S. I. KIM, and F. E. C. CULICK 1990 *Combustion Science and Technology* **72**. Triggering of longitudinal pressure oscillations in combustion chambers. I: nonlinear gasdynamics.
13. E. AWAD and F. E. C. CULICK 1986 *Combustion Science and Technology* **46**. On the existence and stability of limit cycles for longitudinal acoustic modes in combustion chambers.
14. J. WICKER, W. GREENE, S. KIM, and V. YANG 1996 *Journal of Propulsion Power* **12**. Triggering of longitudinal combustion instabilities in rocket motors: nonlinear combustion response.
15. A. DOWLING 1997 *Journal of Fluid Mechanics* **346**. Nonlinear self excited oscillations of a ducted flame.
16. B. T. ZINN and E. A. POWELL 1970 *Proceedings of the 19th International Astronautical Congress*, Vol. 3. Application of the Galerkin method in the solution of combustion instability problems.
17. B. T. ZINN and E. A. POWELL 1970 *Thirteenth (International) Symposium on Combustion. The Combustion Institute, Pittsburgh*. Nonlinear combustion instability in liquid propellant rocket engines.
18. D. HARRJE and F. REARDON 1972 *NASA SP-194*. Liquid propellant rocket combustion instability.
19. J. D. STERLING and E. E. ZUKOSKI 1991 *Combustion Science and Technology* **77**. Nonlinear dynamics of laboratory combustor pressure oscillations.
20. J. D. STERLING 1993 *Combustion Science and Technology* **89**. Nonlinear analysis and modeling of combustion instabilities in a laboratory combustor.
21. R. KEANINI, K. YU and J. DAILY 1989 *American Institute of Aeronautics and Astronautics Paper # 89-0624*. Evidenced of a strange attractor in Ramjet combustion.
22. T. LIEUWEN and B. T. ZINN 2000 *American Institute of Aeronautics and Astronautics Paper # 2000-0707*. Experimental investigation of limit cycle oscillations in an unstable gas turbine combustor.
23. J. W. DAILY 1988 *Combustion Science and Technology* **57**. Cycle to cycle variations: a chaotic process?
24. F. E. C. CULICK, L. PAPARIZOS, J. STERLING and V. BURNLEY 1992 *Proceedings of AGARD Conference on Combat Aircraft Noise. AGARD CP 512*. Combustion noise and combustion instabilities in propulsion systems.
25. V. BURNLEY 1996 *Ph.D. Thesis, California Institute of Technology*. Nonlinear combustion instabilities and stochastic sources.
26. M. BARBER and B. NINHAM 1970 *Random and Restricted Walks*. New York: Gordon and Breach.

APPENDIX A: NOMENCLATURE

A	random process, see equation (3)
C	autocorrelation
d	phase drift (s)
j	number of cycles
k	number of ensemble averages
M	random process, see equation (3)

n	number of cycles in an ensemble
N	total number of cycles of oscillation
q	phase drift (deg)
T	period of oscillations
u	mean inlet velocity

Greek letters

σ	standard deviation